AFRL-IF-RS-TR-2007-160
Final Technical Report
June 2007

SCALABLE VIDEO TRANSMISSION OVER MULTI-RATE MULTIPLE ACCESS CHANNELS

State University of New York at Buffalo

APPROVED FOR PUBLIC RELEASE; DISTRIBUTION UNLIMITED.

STINFO COPY

AIR FORCE RESEARCH LABORATORY
INFORMATION DIRECTORATE
ROME RESEARCH SITE
ROME, NEW YORK

NOTICE AND SIGNATURE PAGE

AFRL-IF-RS-TR-2007-160 HAS BEEN REVIEWED AND IS APPROVED FOR PUBLICATION IN ACCORDANCE WITH ASSIGNED DISTRIBUTION STATEMENT.

FOR THE DIRECTOR:

/s/ /s/

STEPHEN P. REICHHART
Work Unit Manager

WARREN H. DEBANY, Jr.
Technical Advisor, Information Grid Division
Information Directorate

REPORT DOCUMENTATION PAGE

Form Approved
OMB No. 0704-0188

1. REPORT DATE *(DD-MM-YYYY)*	2. REPORT TYPE	3. DATES COVERED *(From - To)*
JUN 2007	Final	Mar 04 – Mar 07

4. TITLE AND SUBTITLE

SCALABLE VIDEO TRANSMISSION OVER MULTI-RATE MULTIPLE ACCESS CHANNELS

5a. CONTRACT NUMBER

5b. GRANT NUMBER
FA8750-04-1-0057

5c. PROGRAM ELEMENT NUMBER
62702F

6. AUTHOR(S)

Lisimachos P. Kondi

5d. PROJECT NUMBER
CITE

5e. TASK NUMBER
UB

5f. WORK UNIT NUMBER
04

7. PERFORMING ORGANIZATION NAME(S) AND ADDRESS(ES)
State University of NY at Buffalo
The Research Foundation
STE 211 UB CMMS 521 Lee E
Amherst NY 14260-0001

8. PERFORMING ORGANIZATION REPORT NUMBER

9. SPONSORING/MONITORING AGENCY NAME(S) AND ADDRESS(ES)

AFRL/IFGC
525 Brooks Rd
Rome NY 13441-4505

10. SPONSOR/MONITOR'S ACRONYM(S)

11. SPONSORING/MONITORING AGENCY REPORT NUMBER
AFRL-IF-RS-TR-2007-160

12. DISTRIBUTION AVAILABILITY STATEMENT
APPROVED FOR PUBLIC RELEASE; DISTRIBUTION UNLIMITED. PA# 07-335

13. SUPPLEMENTARY NOTES

14. ABSTRACT
This effort demonstrated the interference mitigation capabilities of the auxiliary vector (AV) receiver for video transmission over direct-sequence code division multiple access (DS-CDMA) systems. The proposed receiver design is compared to the conventional RAKE matched-filter (RAKE-MF) and sample-matrix-inversion minimum-variance-distortionless-response (SMI-MVDR) receivers. The DS-CDMA video data stream is transmitted over an RF channel under realistic Rayleigh-faded multipath channel conditions, emulating open and/or urban battlefield environments.

15. SUBJECT TERMS
Multipath channel modeling, Auxiliary filtering, Scalable video, spread-spectrum communications

16. SECURITY CLASSIFICATION OF:			17. LIMITATION OF ABSTRACT	18. NUMBER OF PAGES	19a. NAME OF RESPONSIBLE PERSON
a. REPORT	b. ABSTRACT	c. THIS PAGE			Stephen Reichhart
U	U	U	UL	20	19b. TELEPHONE NUMBER (*Include area code*)

Scalable Video Transmission over Multi-Rate Multiple Access Channels

Lisimachos P. Kondi

June 5, 2007

Abstract

In this project, we use a hardware testbed to demonstrate the interference mitigation capabilities of the auxiliary vector (AV) receiver for video transmission over direct-sequence code division multiple access (DS-CDMA) systems. The proposed receiver design is compared to the conventional RAKE matched-filter (RAKE-MF) and sample-matrix-inversion minimum-variance-distortionless-response (SMI-MVDR) receivers. The DS-CDMA video data stream is transmitted over an RF channel under realistic Rayleigh-faded multipath channel conditions, emulating open and/or urban battlefield environments. The state-of-the-art Agilent E4438C RF Arbitrary Waveform Generator and the N115A Baseband Studio fader hardware/software package is used to provide a configurable "real-time" RF channel. In this work, the "foreman" video sequence is source encoded using a MPEG-4 compatible video codec and channel encoded using Rate-Compatible Punctured Convolutional (RCPC) codes. After spreading and modulating, the resultant bitstream is transmitted over a user-defined wireless channel environment created by Agilent equipment. Upon chip-matched filtering and sampling at the chip-rate on a hardware testbed, the received data is despread and demodulated using the AV, RAKE-MF and SMI-MVDR receivers. The resulting data is then channel and source decoded to recover the original transmitted video sequence. The results from this work show that the AV receiver outperforms the RAKE-MF and SMI-MVDR receiver counterparts over a wide range of rates and channel conditions.

Contents

List of Figures

List of Tables

1 INTRODUCTION

In the last few years, there has been a significant amount of research in the area of multimedia communication over direct sequence-code division multiple access (DS-CDMA) channels. In this paper we consider multiuser video transmission over a realistic DS-CDMA multipath fading channel environment created by hardware equipment, and we demonstrate the interference suppression capabilities of the auxiliary-vector (AV) receiver for such systems. The choice of the AV receiver is dictated by realistic channel fading rates that limit the data record available for receiver adaptation and redesign. Under small sample support adaptation, the AV filter short-data-record estimators have been shown to exhibit superior bit-error-rate performance in comparison with least-mean-squares (LMS), recursive-least-squares (RLS), sample-matrix-inversion (SMI), diagonally loaded SMI, or multistage nested Wiener filter implementations [1], [2], [3].

In [4], video transmission from one transmitter to one receiver using binary phase-shift-keying (BPSK) modulation was analyzed. The channel behavior was modeled as non-frequency-selective Rayleigh fading. In [5], video transmission over a DS-CDMA link was considered. A frequency-selective (multipath) Rayleigh fading channel model was used. At the receiver, an adaptive antenna array auxiliary-vector (AV) linear filter that provides space-time RAKE-type processing (thus, taking advantage of the multipath characteristics of the channel) and multiple-access interference suppression was employed [1]. The tradeoffs of source coding, channel coding and spreading for image transmission in CDMA systems were considered in [6]. In [7] and [8], video transmission via a single-rate CDMA channel was compared against transmission via a combination of multi-code multirate CDMA and variable sequence length multirate CDMA under frequency selective Rayleigh fading. In [9], an adaptive video transmission scheme that allocates bandwidth among source coding, channel coding, and spreading to a CDMA network under a fixed constraint on the total bandwidth was presented. A joint optimization method was proposed in [10] for power and transmission rate allocation over multiple CDMA channels as well as joint optimization of Reed-Solomon source/parity rate allocation and RCPC code rate protection for each channel to minimize the distortion of the received video data. In [11], a video sequence was transmitted using the minimum required transmission energy subject to the video quality and delay constraints from the streaming application. In [12], a joint source coding-power control approach was presented that allocates a source coding rate and the energy-per-bit to the multiple-access interference (MAI) density to each user in a CDMA network to maximize the per-cell capacity and the end-to-end QoS for individual users. In [13], a cross-layer optimization technique was proposed that assigns a source coding rate, a channel coding rate, and a power level to all nodes in a DS-CDMA visual sensor network using the MPEG-4 video codec.

In this project, the RF channel environment is created by a hardware testbed unlike previous work in wireless video transmission which usually relied on software simulations of RF channels. The "Foreman" video sequence is source encoded using the MPEG-4 video codec. The source encoded bitstream is then channel encoded with Rate Compatible Punctured Convolutional (RCPC) codes using a particular channel coding rate. The channel coded information is then spread using a Walsh-Hadamard spreading code and carrier modulated for transmission over the wireless channel. In order to emulate open and/or urban battlefield environments, the transmission over a RF channel with Rayleigh-faded multipath channel conditions is accomplished by passing the spread data through the Agilent E4438C Vector Signal Generator and Baseband Studio Fader. At the receiver, the information is demodulated and despread using the AV filter, RAKE-MF filter, or SMI-MVDR filter. The despread data is then channel decoded using the Viterbi decoder. Finally, the original "Foreman" video sequence is reconstructed using the MPEG-4 source decoder.

The rest of this report is organized as follows: in Section 2, we describe the components of the

proposed video transmission system, i.e., source coding in Section 2.1, "packetization" in Section 2.2, interleaving in Section 2.3, channel encoding in Section 2.4, spreading in Section 2.5, channel modeling in Section 2.6, the received signal model in Section 2.7, and Auxiliary Vector (AV) filtering in Section 2.8. Experimental results are presented in Section 3, and conclusions are drawn in Section 4.

2 VIDEO TRANSMISSION SYSTEM

The proposed video transmission system is shown in Figure 1. The system is composed of source encoding with the MPEG-4 video codec, "packetization", interleaving, channel encoding with RCPC codes, spreading with Walsh-Hadamard codes, transmission over a RF channel created by a hardware testbed, despreading with the AV filter, channel decoding with the Viterbi algorithm, "depacketization", and source decoding with the MPEG-4 video codec.

2.1 Source Coding

Video source coding is a technique for compressing video data. There are several standards that specify the way source coding can be carried out and the syntax of the resulting bitstream. In this work, an MPEG-4 compatible video source codec is used for video source coding. MPEG-4 is a standard for multimedia applications which became an international standard with the ISO number 14496 [14] with a video verification model [15]. Codecs based on MPEG-4 are also block-based hybrid codecs using the Discrete Cosine Transform (DCT) as the earlier standards such as H.261, H.263, H.263+, MPEG-1/2. However, it differs from the earlier codecs with its content-based functionalities while the earlier standards had a frame as the coding unit. The general block schematic of a block-based hybrid MPEG-4 video codec is shown in Fig. 2 while the corresponding decoder is shown in Fig. 3. The error-resilience tools of MPEG-4 such as resynchronization markers, data partitioning and reversible variable length codes (RVLCs) were enabled to produce an efficient transmission of video.

Resynchronization markers (resync markers) are a unique string of bits inserted by the encoder periodically in the bitstream. If syncronization is lost at the decoder due to channel errors, the decoder searches for the next resync marker and continues decoding. Resync markers are inserted when the number of bits in the bitstream since the last resync marker exceeds a predetermined value. The value used for this spacing is dependent on the anticipated error conditions of the transmission channel and the compressed data rate. The ISO/IEC committee has suggested values for this spacing for low bit rates while at higher rates, they are to be determined. Apart from the *resync marker* field, the encoder also inserts a field to indicate the current macroblock address, the current quantization parameter (QP) and Header Extension Code (HEC).

In the data partitioning mode, a *motion marker* field is inserted after the motion data apart from the *resync marker* fields, MB address, QP and HEC. This *motion marker* field is distinct from the motion data and helps the decoder determine whether all the motion information has been received correctly.

Codewords produced by an entropy coder are of variable length leading to Variable Length Codes (VLC). The use of reversible VLCs (RVLCs) enables the decoder to recover additional texture information in the presence of errors. This is accomplished by first detecting the error and searching forward to the next *resync marker*. Once this point is determined the texture data can be read in the reverse direction until an error is detected. When errors are detected in the texture data, the decoder can use the correctly decoded motion vector information to perform

motion compensation and conceal these errors. An example of a portion of a bit stream with *resync marker* and RVLCs is shown in Figure 4.

2.2 Packetization

The source encoded video bitstream is then "packetized" by breaking the bitstream up into blocks before performing interleaving and channel encoding on. At the receiver, the stream is then "depacketized" by combining the blocks after channel decoding and deinterleaving into one continuous bitstream.

2.3 Interleaving

The performance of channel coding can be improved by using an interleaver in addition to an error correcting code. An interleaver is a software technique that mixes up symbols from different codewords so that consecutive symbols within the same codeword are spread across several codewords. The effect of the interleaver is to increase the probability that error bursts would affect different symbols belonging to different codewords.

At the decoder, a deinterleaver is used to restore the symbols back to their original codewords. The interleaver/deinterleaver pair has the effect of randomizing burst errors seen by the channel decoder. The decoder can perform decoding as if the received data has gone through a random error channel instead of a burst error channel.

2.4 Channel Coding

In this work, we use RCPC codes for channel coding. With convolutional coding, the source data is convolved with a convolutional matrix $\mathbf{G}$, which specifies which delayed inputs to add to the current input. This process is equivalent to passing the input data through a linear finite-state register where the tap connections are defined by $\mathbf{G}$. Unlike linear block codes that have a number of channel code symbols for a corresponding block of source symbols, convolutional coding generates one codeword for the entire source data. Convolution is the process of modulo-2 addition of the current source bit with previously delayed source bits. This is analogous to passing the input through a linear finite-state register where the tap connections are defined by the generator matrix. The rate of the convolutional code is defined as k/n where k is the number of input bits and n is the number of output bits.

The Viterbi algorithm is used to decode convolutional codes. This algorithm is a maximum-likelihood sequence estimation procedure [16]. The two types of Viterbi decoding are soft and hard decision decoding. In soft decision decoding, decision statistics of the channel output are passed to the decoder. Usually, the distortion metric used is the Euclidean distance. In hard decision decoding, the decision of the received bit is made before the received data is input into the Viterbi decoder. The distortion metric commonly used for hard decision decoding is the Hamming distance [17].

Punctured convolutional codes were originally developed to simplify Viterbi decoding for rate k/n with two branches arriving at each node instead of 2^k branches. Puncturing is the process of deleting bits from the output sequence in a predefined manner so that fewer bits are transmitted than in the original code. The idea of puncturing was extended to include the concept of rate compatibility. Rate compatibility requires that a higher-rate code be a subset of a lower-rate code, or that lower-protection codes be embedded into higher-protection codes. This is accomplished by puncturing a "mother" code of rate $1/n$ to achieve higher rates. One major benefit of these RCPC codes with the same mother code is that they all can be decoded by the same Viterbi decoder [18].

2.5 Spreading

This work considers a wireless video transmission system that utilizes DS-CDMA. DS-CDMA channels allow several users to use the same frequency band at the same time. Users' transmissions are distinguished through the use of different spreading codes. But even if the spreading codes used are orthogonal to each other, as with the Walsh-Hadamard code set, transmissions of one user cause interference to the other users, due to possible asynchronous transmissions and multipath fading. In this DS-CDMA system, the data is spread after channel decoding using a Walsh-Hadamard spreading code and is then carrier-modulated.

2.6 Channel Modeling

The Agilent E4438C RF Arbitrary Waveform Generator and the N115A Baseband Studio fader hardware/software package were used to create a "real time" RF Rayleigh fading channel with multipath and Doppler frequencies. The E4438C RF Waveform Generator converts baseband I/Q data to RF. The N115A Baseband Studio obtains non-faded I/Q data from the E4438C arbitrary waveform generator. Based on operator selected fading parameters, it computes and inserts faded I/Q data, in "real-time", back into the waveform generator. This setup is used to emulate open and/or urban battlefield environments with up to 48 paths and various Doppler frequencies.

2.7 Received Signal

We model the baseband received signal as the aggregate of the received multipath DS-CDMA signal-of-interest with signature code $\mathbf{S}_o$ of length L, $K-1$ received DS-CDMA interferers with signatures $\mathbf{S}_k$, $k = 1, ..., K-1$, and white Gaussian noise. If T is the symbol period and T_c is the chip period then $L = T/T_c$. For notational simplicity and without the loss of generality, we choose a chip-synchronous signal set-up. We assume that the multipath spread is on the order of a few chip intervals, P. Since the signal is bandlimited to $B = 1/2T_c$, the lowpass channel can be represented as a tapped delay line with $P+1$ taps spaced at chip intervals, T_c. After conventional chip-matched filtering and sampling at the chip rate over a multipath-extended symbol interval of $L+P$ chips, the $L+P$ data samples can be represented in the form of a vector, $\mathbf{r}$, given by

$$\mathbf{r} = \sum_{k=0}^{K-1} \sum_{p=0}^{P} c_{k,p} \sqrt{E_k} (b_k \mathbf{S}_{k,p} + b_k^- \mathbf{S}_{k,p}^- + b_k^+ \mathbf{S}_{k,p}^+) + \mathbf{n} \tag{1}$$

where E_k is the transmitted energy, b_k, b_k^-, b_k^+ are the present, the previous and the following transmitted bits, respectively, and $\{c_{k,p}\}$ are the coefficients of the Rayleigh fading multipath channel created by the Agilent E4438C Vector Signal Generator and N115A Baseband Studio Fader. $\mathbf{S}_{k,p}$ represents the zero-padded by P, p-cyclic-shifted version of the signature of the kth DS-CDMA signal $\mathbf{S}_k$, $\mathbf{S}_{k,p}^-$ is the 0-filled $(L-p)$-left-shifted version of $\mathbf{S}_{k,0}$ and $\mathbf{S}_{k,p}^+$ is the 0-filled $(L-p)$-right-shifted version of $\mathbf{S}_{k,0}$, and $\mathbf{n}$ is the additive complex Gaussian noise. For conceptual and notational simplicity we may rewrite the received data equation as follows

$$\mathbf{r} = \sqrt{E_0} b_0 \mathbf{w}_{R-MF} + \mathbf{I} + \mathbf{n} \tag{2}$$

where is $\mathbf{w}_{R-MF}$ is the RAKE Matched-Filter and $\mathbf{I}$ identifies comprehensively both the Inter-Symbol and the DS-CDMA interference present in $\mathbf{r}$. In this work, as the fading coefficients are not known, $E_{b_0}\{.\}$, the statistical expectation with respect to b_0 is used to estimate $\mathbf{w}_{R-MF}$. This is done by using pilot bits from the DS-CDMA signal of interest which are assumed to be available

at the receiver error-free. The effective channel-processed signature, the RAKE Matched-Filter, of the DS-CDMA signal-of-interest is given by

$$\mathbf{w}_{R-MF} = E_{b_0}\{\mathbf{r}b_0\} = \sum_{p=0}^{P} c_{0,p}\mathbf{S}_{0,p} \tag{3}$$

2.8 Auxiliary-Vector Adaptive Filtering

After carrier demodulation, chip-matched filtering, and chip-rate sampling, auxiliary-vector (AV) filtering provides Multiple-Access-Interference (MAI) suppressing despreading. The AV receiver was chosen based on the realistic channel fading rates that limit the data record available for receiver adaptation. Under small sample support adaptation, AV filter short-data-record estimators have been shown to exhibit superior bit error rate (BER) performance in comparison to least mean squares (LMS), recursive least squares (RLS), sample matrix inversion (SMI), diagonally-loaded SMI, or multistage nested Wiener filter implementations [2], [3]. The AV algorithm generates a sequence of AV filters making use of two basic principles: (i) The maximum magnitude cross-correlation criterion for the evaluation of the auxiliary vectors (ii) The conditional mean-squared optimization criterion for the evaluation of the scalar AV weights. The AV algorithm generates an infinite sequence of filters $\{\mathbf{w}_k\}_{k=0}^{\infty}$. The sequence is initialized at the S-T RAKE filter

$$\mathbf{w}_0 = \frac{\mathbf{w}_{\text{R-MF}}}{\|\mathbf{w}_{\text{R-MF}}\|^2}, \tag{4}$$

which is here scaled to satisfy $\mathbf{w}_0^H\mathbf{w}_{\text{R-MF}} = 1$. At each step $k+1$ of the algorithm, $k = 0, 1, 2, \ldots$, an "auxiliary" vector component $\mathbf{g}_{k+1}$ that is orthogonal to $\mathbf{w}_{\text{R-MF}}$ is incorporated in $\mathbf{w}_k$ and weighted by a scalar μ_{k+1} to form the next filter in the sequence,

$$\mathbf{w}_{k+1} = \mathbf{w}_k - \mu_{k+1}\mathbf{g}_{k+1}. \tag{5}$$

The auxiliary vector $\mathbf{g}_{k+1}$ is chosen to maximize, under fixed norm, the magnitude of the cross-correlation between its output, $\mathbf{g}_{k+1}^H\mathbf{r}$, and the previous filter output, $\mathbf{w}_k^H\mathbf{r}$, and is given by

$$\mathbf{g}_{k+1} = \mathbf{R}\mathbf{w}_k - \frac{\mathbf{w}_{\text{R-MF}}^H\mathbf{R}\mathbf{w}_k}{\|\mathbf{w}_{\text{R-MF}}\|^2}\mathbf{w}_{\text{R-MF}} \tag{6}$$

where $\mathbf{R}$ is the input autocorrelation matrix, $\mathbf{R} = E\{\mathbf{r}\mathbf{r}^H\}$. The scalar μ_{k+1} is selected such that it minimizes the output variance of the filter $\mathbf{w}_{k+1}$ or equivalently minimizes the mean-square (MS) error between $\mathbf{w}_k^H\mathbf{r}$ and $\mu_{k+1}^*\mathbf{g}_{k+1}^H\mathbf{r}$. The MS-optimum μ_{k+1} is

$$\mu_{k+1} = \frac{\mathbf{g}_{k+1}^H\mathbf{R}\mathbf{w}_k}{\mathbf{g}_{k+1}^H\mathbf{R}\mathbf{g}_{k+1}}. \tag{7}$$

The AV filter recursion is completely defined by (4)-(7). Theoretical analysis of the AV algorithm was pursued in [1]. The results are summarized below in the form of a theorem.

Theorem 1 *Let* $\mathbf{R}$ *be a Hermitian positive definite matrix. Consider the iterative algorithm of eqs. (4)-(7).*
(i) Successive *auxiliary vectors generated through (5)-(7) are orthogonal:* $\mathbf{g}_k^H\mathbf{g}_{k+1} = 0$, $k = 1, 2, 3, \ldots$ *(however, in general* $\mathbf{g}_k^H\mathbf{g}_j \neq 0$ *for* $|k-j| \neq 1$*).*
(ii) The generated sequence of auxiliary-vector weights $\{\mu_k\}$, $k = 1, 2, \ldots$, *is real-valued, positive,*

and bounded: $0 < \frac{1}{\lambda_{\max}} \leq \mu_k \leq \frac{1}{\lambda_{\min}}$, $k = 1, 2, \ldots$, *where* $\lambda_{\max}$ *and* $\lambda_{\min}$ *are the maximum and minimum, correspondingly, eigenvalues of* $\mathbf{R}$.
(iii) The sequence of auxiliary vectors $\{\mathbf{g}_k\}$, $k = 1, 2, \ldots$, *converges to the* $\mathbf{0}$ *vector:* $\lim_{n\to\infty} \mathbf{g}_n = \mathbf{0}$.
(iv) The sequence of auxiliary-vector filters $\{\mathbf{w}_k\}$, $k = 1, 2, \ldots$, *converges to the minimum-variance-distortionless-response (MVDR) filter:* $\lim_{k\to\infty} \mathbf{w}_k = \frac{\mathbf{R}^{-1}\mathbf{w}_{R\text{-}MF}}{\mathbf{w}_{R\text{-}MF}^H \mathbf{R}^{-1}\mathbf{w}_{R\text{-}MF}}$. □

If $\mathbf{R}$ is unknown and sample-average estimated from a packet data record of D points, $\hat{\mathbf{R}}(D) = \frac{1}{D}\sum_{d=1}^{D} \mathbf{r}_d \mathbf{r}_d^H$, then Theorem 1 shows that

$$\hat{\mathbf{w}}_k(D) \underset{k\to\infty}{\longrightarrow} \hat{\mathbf{w}}_\infty(D) = \frac{\left[\hat{\mathbf{R}}(D)\right]^{-1}\mathbf{w}_{\text{R-MF}}}{\mathbf{w}_{\text{R-MF}}^H \left[\hat{\mathbf{R}}(D)\right]^{-1}\mathbf{w}_{\text{R-MF}}} \tag{8}$$

where $\hat{\mathbf{w}}_\infty(D)$ is the widely used MVDR filter estimator known as the sample-matrix-inversion (SMI) filter [19]. The output sequence begins from $\hat{\mathbf{w}}_0(D) = \frac{\mathbf{w}_{\text{R-MF}}}{\|\mathbf{w}_{\text{R-MF}}\|^2}$, which is a *0*-variance, fixed-valued, estimator that may be severely biased ($\hat{\mathbf{w}}_0(D) = \frac{\mathbf{w}_{\text{R-MF}}}{\|\mathbf{w}_{\text{R-MF}}\|^2} \neq \mathbf{w}_{\text{MVDR}}$) unless $\mathbf{R} = \sigma^2\mathbf{I}$ for some $\sigma > 0$. In the latter trivial case, $\hat{\mathbf{w}}_0(D)$ is already the perfect MVDR filter. Otherwise, the next filter estimator in the sequence, $\hat{\mathbf{w}}_1(D)$, has a significantly reduced bias due to the optimization procedure employed at the expense of non-zero estimator (co-)variance. As we move up in the sequence of filter estimators $\hat{\mathbf{w}}_k(D)$, $k = 0, 1, 2, \ldots$, the bias decreases rapidly to zero while the variance rises slowly to the SMI ($\hat{\mathbf{w}}_\infty(D)$) levels (cf. (8)).

An adaptive data-dependent procedure for the selection of the most appropriate member of the AV filter estimator sequence $\{\hat{\mathbf{w}}_k(D)\}$ for a given data record of size D is presented in [20]. The procedure selects the estimator $\hat{\mathbf{w}}_k$ from the generated sequence of AV filter estimators that exhibits maximum J-divergence between the filter output conditional distributions given that $+1$ or -1 is transmitted. Under a Gaussian approximation on the conditional filter output distribution, it was shown in [20] that the J-divergence of the filter estimator with k auxiliary vectors is

$$J(k) = \frac{4\,E^2\left\{b_0 \text{Re}\left[\hat{\mathbf{w}}_k^H(D)\mathbf{r}\right]\right\}}{Var\left\{b_0 \text{Re}\left[\hat{\mathbf{w}}_k^H(D)\mathbf{r}\right]\right\}}. \tag{9}$$

To estimate the J-divergence $J(k)$ from the data packet of size D, the transmitted information bits b_0 are required to be known. A blind *approximate* version of $J(k)$ can be obtained by substituting the information bit b_0 in (9) by the detected bit $\hat{b}_0 = \text{sgn}\left(\text{Re}\left\{\hat{\mathbf{w}}_k^H(D)\mathbf{r}\right\}\right)$ (output of the sign detector that follows the linear filter). In particular, using $\hat{b}_0$ in place of b_0 in (9) gives the following J-divergence expression:

$$J_B(k) = \frac{4\,E^2\left\{\hat{b}_0 \text{Re}\left[\hat{\mathbf{w}}_k^H(D)\mathbf{r}\right]\right\}}{Var\left\{\hat{b}_0 \text{Re}\left[\hat{\mathbf{w}}_k^H(D)\mathbf{r}\right]\right\}} = \frac{4\,E^2\left\{\left|\text{Re}\left[\hat{\mathbf{w}}_k^H(D)\mathbf{r}\right]\right|\right\}}{Var\left\{\left|\text{Re}\left[\hat{\mathbf{w}}_k^H(D)\mathbf{r}\right]\right|\right\}} \tag{10}$$

where the subscript B identifies the blind version of the J-divergence function. To estimate $J_B(k)$ from the data packet of size, D, we substitute the statistical expectations in (10) by sample averages. The following criterion summarizes the corresponding AV filter estimator selection rule.

Criterion 1 *For a given data record of size, D, the unsupervised (blind) J-divergence AV filter estimator selection rule chooses the estimator* $\hat{\mathbf{w}}_k(D)$ *with k auxiliary vectors where*

$$k = \arg\max_k \left\{\hat{J}_B(k)\right\} = \arg\max_k \left\{\frac{4\left[\frac{1}{D}\sum_{d=1}^{D}\left|\text{Re}\left[\hat{\mathbf{w}}_k^H(D)\mathbf{r}_d\right]\right|\right]^2}{\frac{1}{D}\sum_{d=1}^{D}\left|\text{Re}\left[\hat{\mathbf{w}}_k^H(D)\mathbf{r}_d\right]\right|^2 - \left[\frac{1}{D}\sum_{d=1}^{D}\left|\text{Re}\left[\hat{\mathbf{w}}_k^H(D)\mathbf{r}_d\right]\right|\right]^2}\right\}. \tag{11}$$

□

Table 1: Simulation results for 150 frame video sequence encoded at 120 kbps with zero Doppler.

Filter Type	Block Size	Pilot Bit %	BER	Total Frames Decoded
AV	410	12	1.40E-05	54
RAKE-MF	410	12	6.33E-02	0
SMI-MVDR	410	12	4.20E-03	0
AV	410	13	3.10E-06	150 (ALL)
RAKE-MF	410	13	5.90E-02	0
SMI-MVDR	410	13	5.77E-04	0

Criterion 1 completes the design of the joint S-T auxiliary-vector filter estimator.

3 EXPERIMENTAL RESULTS

In this section, we present the experimental results for the setup described above. We assume $K = 7$ users that employ DS-CDMA signaling, the user-of-interest and six interferers. As a result of the limitations of the hardware used to create the RF channel environment, only one user could be transmitted over the channel at a time. To provide the more realistic multiuser scenario, individual user data was summed at the receiver. An MPEG-4 compatible source codec was used to encode a "Foreman" video sequence with two different source coding rates of 40 and 120 kbps. RCPC codes were used for channel coding by using a "mother" code rate of 1/4 and puncturing it down to the code rate of 1/2. Walsh-Hadamard codes of length $L = 16$ were used as spreading codes. The transmission over a Rayleigh fading channel was emulated by the Agilent RF Waveform Generator and Baseband Studio Fader with all DS-CDMA signals, $k = 0, 1, \ldots, K-1$, experiencing $P = 3$ resolvable multipaths and various Doppler values equal to 0, 4, 40 or 200 Hz.

Three different receivers were assumed: The RAKE matched-filter (RAKE-MF), the conventional sample-matrix-inversion minimum-variance-distortionless-response (SMI-MVDR) filter, and the auxiliary vector (AV) filter. Based on Criterion 1 given in Section 2.8, the best AV was selected out of 11 AV's that were produced. The channel decoding was performed by utilizing the Viterbi algorithm with hard-decision decoding, and the source decoding was completed by using the MPEG-4 video codec.

The tabulated results obtained by this study are shown next. The resulting video quality of all the decoded frames is comparable, so the measure by which the output is deemed superior is the number of frames that can be decoded. And, if there are multiple sets that produce video clips in which all frames can be decoded, the best set is determined by the lowest number of pilot bits necessary. The amount of pilot bits is measured as a percentage of the bits per block used. The block size in the tables below refer to the size of the block after channel encoding. For all the cases, the bit error rate (BER) is calculated after channel decoding is completed at the receiver.

Table 1 gives the results for the cases where there is zero Doppler. It corresponds to the simulations run with the 150-frame video sequence encoded at the rate of 120 kbps. When using 13% or 12% of the block size, 410, as pilot bits, the AV filter recovers frames from the video sequence. For the same packet size and number of pilot bits, the RAKE-MF and the SMI-MVDR filter can not even produce any decodable video frames.

The results for the case where only the user-of-interest experiences Doppler shifts of 4 Hz while the interfering users experience zero Doppler are given in Table 2. The block sizes were adjusted

Table 2: Simulation results for 300 frame video sequence encoded at 40 kbps using the AV filter: User-of-interest experiences 4Hz Doppler but the interferers experience zero Doppler

Filter Type	Block Size	Pilot Bit %	BER	Total Frames Decoded
AV	810	7.5	0	300 (ALL)
RAKE-MF	810	7.5	4.68E-02	0
SMI-MVDR	810	7.5	1.09E-04	0
AV	810	10	0	300 (ALL)
RAKE-MF	810	10	2.54E-02	0
SMI-MVDR	810	10	3.24E-05	300 (ALL)

Table 3: Simulation results for 300 frame video sequence encoded at 40 kbps using the AV filter: User-of-interest experiences Doppler but the interferers experience zero Doppler

Doppler	Block Size	Pilot Bit %	BER	Total Frames Decoded
0	2010	10	0	300 (ALL)
0	2010	5	0	300 (ALL)
4	810	10	0	300 (ALL)
4	810	7.5	0	300 (ALL)
4	810	5	1.43E-04	0
40	610	10	0	300 (ALL)
40	610	7.5	6.01E-05	134
40	610	5	3.40E-04	0
200	250	12.5	4.62E-06	300 (ALL)
200	250	10	2.48E-04	0

according to the Doppler frequency to maintain the assumption of constant fading over each block. The AV filter gives a fully-decodable video stream with only 7.5% of the block size used as pilot bits while the SMI-MVDR filter requires 10% of the block size to be used for pilot bits to achieve the same results. We see that using the RAKE-MF filter results in the inability to recover any of frames with a practical number of pilot bits.

In Table 3, we vary the Doppler experienced by the user-of-interest while maintaining zero Doppler for the interfering users. The block size is adjusted according to the Doppler shift to keep the same fading coefficients over the entire block. With the zero Doppler case, the performance improves if a larger packet size is used. Even with just 5% of the block size used as pilot bits, the AV filtering technique results in all frames being decoded. The block size may be further increased past 2010, but the computational complexity increases with increasing block size. We saw in Table 2 that in the 4Hz Doppler case, the SMI-MVDR was still able to achieve fully-decodable video if 10% of the block size is used for pilot bits and that RAKE-MF could not recover any frames. When we go to the 40Hz Doppler case, the SMI-MVDR filter required 50% of the block size known at the receiver which is not realistic. And, again RAKE-MF cannot recover any frames even with a large number of pilot bits. And so, we omit SMI-MVDR and RAKE-MF from Table 3. We see that the AV filter can even recover all frames if just 10% and 12.5% of the block size are used as pilot bits, respectively, are used for the 40Hz and 200Hz Doppler cases.

Table 4: Simulation results for 150 frame video sequence encoded at 40 kbps with 4 Hz Doppler

Filter Type	Block Size	Pilot Bit %	BER	Total Frames Decoded
AV	810	10	7.39E-05	70
RAKE-MF	810	10	5.71E-02	0
SMI-MVDR	810	10	1.20E-03	0
AV	810	12.5	4.31E-05	150 (ALL)
RAKE-MF	810	12.5	5.00E-02	0
SMI-MVDR	810	12.5	3.90E-05	0
AV	1010	20	7.18E-06	150 (ALL)
RAKE-MF	1010	20	5.72E-02	0
SMI-MVDR	1010	20	6.74E-05	70
AV	610	25	5.41E-05	150 (ALL)
RAKE-MF	610	25	4.48E-02	0
SMI-MVDR	610	25	1.76E-04	0
AV	276	30	2.15E-05	150 (ALL)
RAKE-MF	276	30	4.97E-02	0
SMI-MVDR	276	30	9.48E-04	0

Table 5: Simulation results for 300 frame video sequence encoded at 40 kbps with 40 Hz Doppler

Filter Type	Block Size	Pilot Bit %	BER	Total Frames Decoded
AV	610	7.5	6.01E-05	134
RAKE-MF	610	7.5	5.80E-02	0
SMI-MDR	610	7.5	6.50E-03	0
AV	610	10	0	300 (ALL)
RAKE-MF	610	10	7.20E-02	0
SMI-MVDR	610	10	1.50E-03	0

Table 4 shows the results for the situation where all users experience the same Doppler shift of 4 Hz. Again, the block sizes are varied to maintain constant fading over each block. There are three cases that produce fully-decodable video using AV filters. However, using 30% of a block size of 276 bits or even 20% of a block size of 1010 bits for pilot bits is not a practical condition. Hence using 12.5% of a block size of 810 bits as pilot bits can be considered as the best choice. Also, neither RAKE-MF filter nor SMI-MVDR filter recovered any part of the video sequence for any reasonable number of pilot bits.

Tables 5 and 6 show the results for 40 and 200 Hz Doppler shifts experienced by all users in the system. We see that the block size must be decreased as the Doppler shifts get higher. The values in these tables clearly show that the AV filter outperforms RAKE-MF and SMI-MVDR filters for a practical number of pilot bits used.

Table 6: Simulation results for 300 frame video sequence encoded at 40 kbps with 200 Hz Doppler

Filter Type	Block Size	Pilot Bit %	BER	Total Frames Decoded
AV	250	12.5	4.62E-06	300 (ALL)
RAKE-MF	250	12.5	5.70E-02	0
SMI-MVDR	250	12.5	2.48E-04	0

4 CONCLUSIONS

We demonstrated the effectiveness of using an Auxiliary Vector (AV) receiver for video transmission over DS-CDMA channels with "real-world" multipath channel conditions created by a hardware testbed. The Agilent E4438C RF Arbitrary Waveform Generator and the N115A Baseband Studio fader hardware/software package were used to create a "real-time" RF Rayleigh fading channel with multipath and Doppler frequencies. In this work, a video sequence is source-encoded using an MPEG-4 video codec and channel-encoded using RCPC codes. After spreading and modulating, the resulting bitstream is transmitted over a user-defined wireless channel emulation. Upon chip-matched filtering and sampling at the chip-rate on a hardware testbed, the received data are despread/demodulated using the AV, RAKE-MF and SMI-MVDR receivers and, subsequently, channel and source decoded. The results clearly establish the interference mitigation capabilities of the AV receiver. The AV filter receiver was also shown to outperform the RAKE-MF and the SMI-MVDR receivers under a wide range of rates and channel conditions.

References

[1] D. A. Pados and G. N. Karystinos, "An iterative algorithm for the computation of the MVDR filter," *IEEE Transactions on Signal Processing*, vol. 49, pp. 290–300, February 2001.

[2] A. Kansal, S. N. Batalama, and D. A. Pados, "Adaptive maximum SINR RAKE filtering and DS-CDMA multipath fading channels," *IEEE Journal on Selected Areas of Communications*, vol. 16, pp. 1765–1773, December 1998.

[3] J. S. Goldstein, I. S. Reed, and L. L. Sharf, "A multistage representation of the Wiener filter based on orthogonal projections," *IEEE Transactions on Image Processing*, vol. 44, pp. 2943–2959, November 1998.

[4] L. P. Kondi, F. Ishtiaq, and A. K. Katsaggelos, "Joint source-channel coding for motion-compensated DCT-based SNR scalable video," *IEEE Transactions on Image Processing*, vol. 11, no. 9, pp. 1043–1052, September 2002.

[5] L. P. Kondi, S. N. Batalama, D. A. Pados, and A. K. Katsaggelos, "Joint source-channel coding for scalable video over DS-CDMA multipath fading channels," in *Proc. of the IEEE International Conference Image Processing*, Thessaloniki, Greece, 2002.

[6] Q. Zhao, P. Cosman, and L. B. Milstein, "Tradeoffs of source coding, channel coding and spreading in CDMA systems," in *Proc. MILCOM*, Los Angeles, USA, 2000, vol. 2, pp. 846–850.

[7] L. P. Kondi, D. Srinivasan, D. A. Pados, and S. N. Batalama, "Layered video transmission over multirate DS-CDMA wireless systems," *IEEE Transactions on Circuits and Systems for Video Technology*, vol. 15, no. 12, pp. 1629–1637, December 2005.

[8] L. P. Kondi, D. Srinivasan, and D. A. Pados, "Scalable video transmission over wireless DS-CDMA channesl using minimum TSC spreading codes," *IEEE Signal Processing Letters*, vol. 11, no. 10, pp. 836–840, October 2004.

[9] Y. Shen, P. C. Cosman, and L. B. Milstein, "Error-resilient video communications over CDMA networks with a bandwidth constraint," *IEEE Transactions on Image Processing*, vol. 15, no. 11, pp. 3241–3252, November 2006.

[10] S. Zhao, Z. Xiong, and X. Wang, "Optimal resource allocation for wireless video over CDMA networks," *IEEE Transactions on Mobile Computing*, vol. 4, no. 1, pp. 56–67, January-February 2005.

[11] C. E. Luna, Y. Eisenberg, R. Berry, T. N. Pappas, and A. K. Katsaggelos, "Joint source coding and data rate adaptation for energy efficient wireless video streaming," *IEEE Journal on Selected Areas in Communications*, vol. 21, no. 10, pp. 1710–1720, December 2003.

[12] Y. S. Chan and J. W. Modestino, "A Joint Source Coding-Power Control Approach for Video Transmission Over CDMA Networks," *IEEE Journal on Selected Areas in Communications*, vol. 21, no. 10, pp. 1516–1525, December 2003.

[13] E. S. Pynadath and L. P. Kondi, "Cross-layer optimization with power control in DS-CDMA visual sensor networks," in *Proc. of the IEEE International Conference on Image Processing*, Atlanta, GA, 2006, pp. 25–28.

[14] ISO/IEC 14496-2 MPEG-4, "Information technology-coding of audio-visual objects: Visual," October, 1997.

[15] International Organization for Standardisation, "MPEG-4 Video Verification Model 5.0," November 1996.

[16] G. D. Forney, "The Viterbi Algorithm," *Proc. IEEE*, vol. 61, pp. 268–278, March 1973.

[17] J. B. Cain, G. C. Clark, and J. M. Geist, "Punctured convolutional codes or rate (n-1)/n and simplified maximum likelihood decoding," *IEEE Transactions on Information Theory*, vol. IT-25, pp. 97–100, 1979.

[18] J. Hagenauer, "Rate-compatible punctured convolutional codes (RCPC codes) and their applications," *IEEE Transactions on Communications*, vol. 36, no. 4, pp. 389–400, April 1988.

[19] I. S. Reed, J. M. Mallet, and L. E. Brennan, "Rapid convergence rate in adaptive arrays," *IEEE Transactions on Aerospace Electronic Systems*, vol. 10, pp. 853–863, November 1974.

[20] H. Qian and S. N. Batalama, "Data-record-based criteria for selection of an auxiliary-vector estimator of the MMSE/MVDR filter," *IEEE Transactions on Communications*, vol. 51, no. 10, pp. 1700–1708, October 2003.

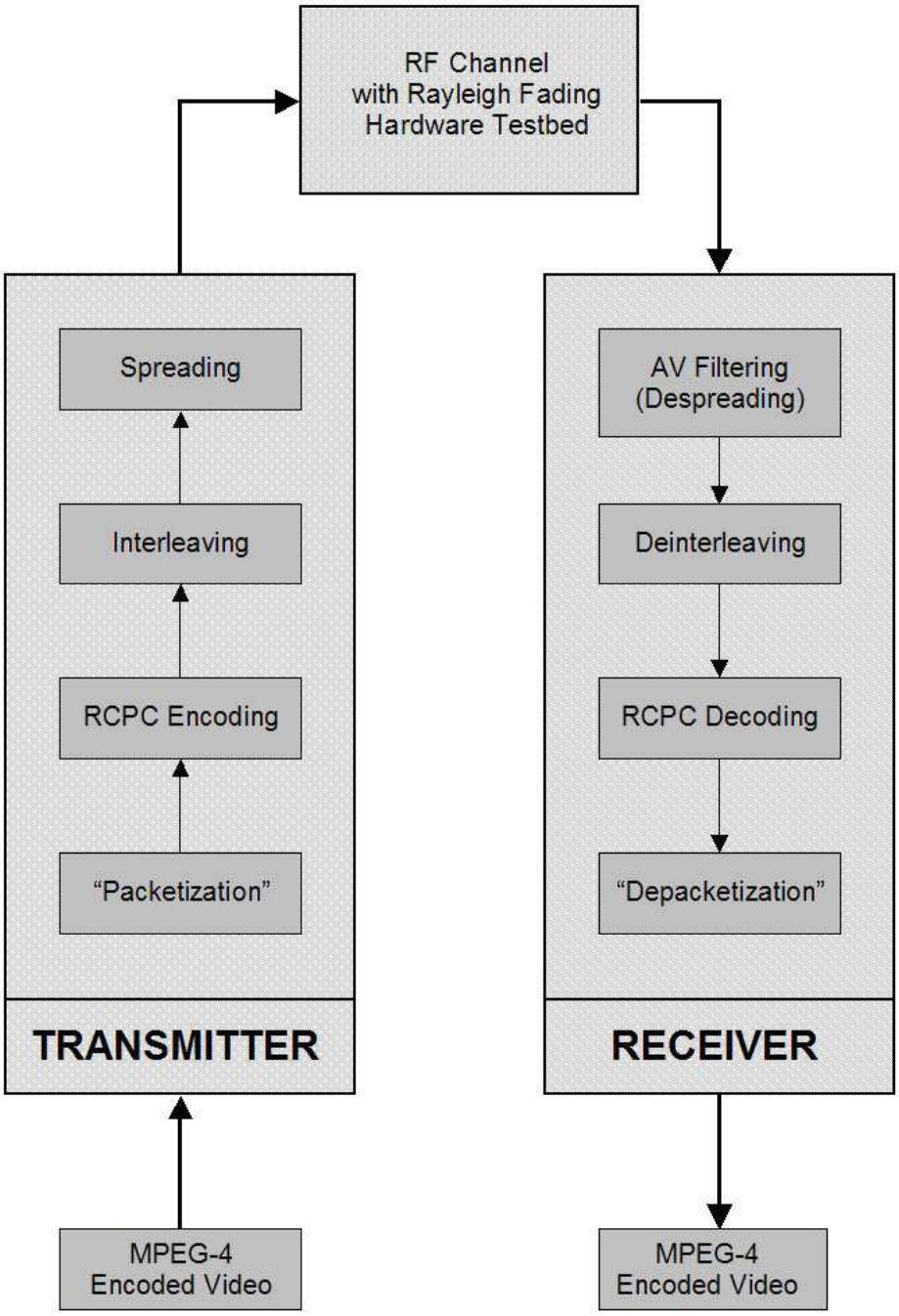

Figure 1: Video Transmission DS-CDMA System.

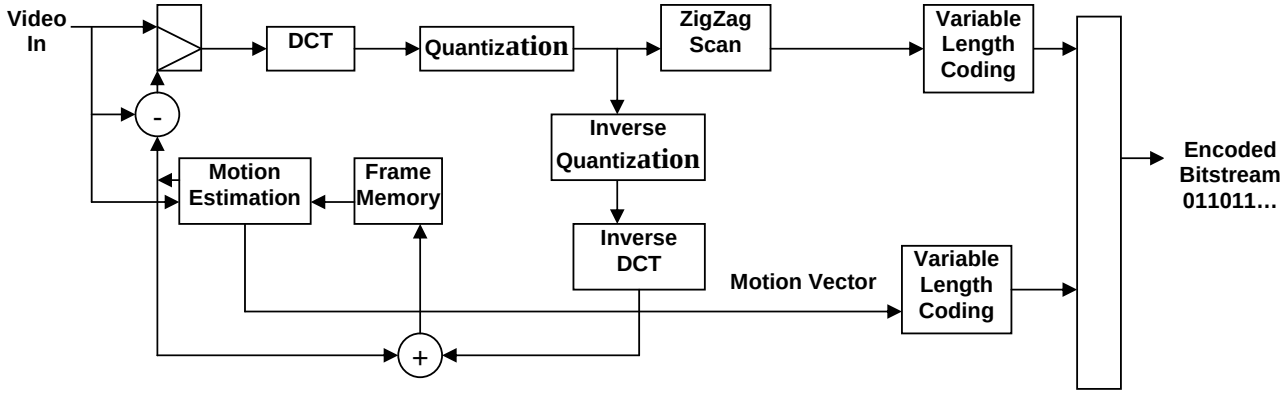

Figure 2: Block-based hybrid MPEG-4 video encoder.

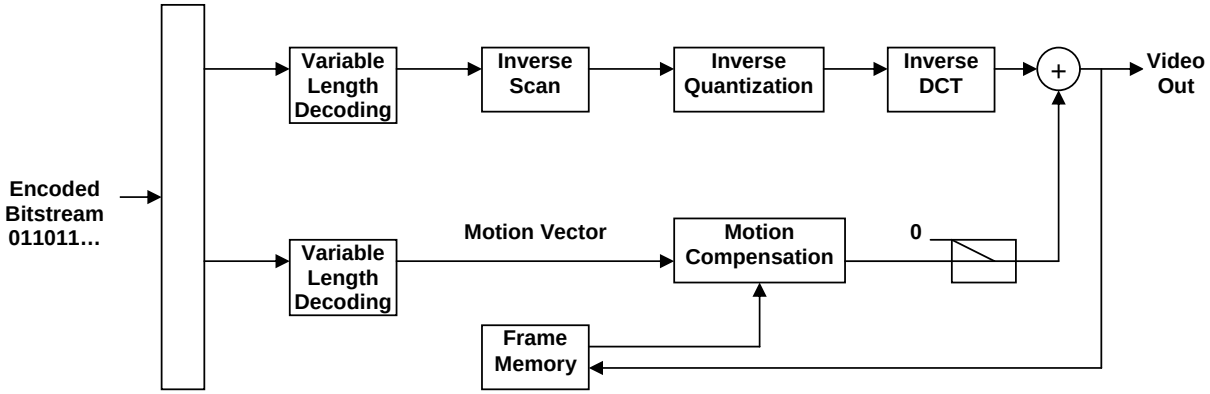

Figure 3: Block-based hybrid MPEG-4 video decoder.

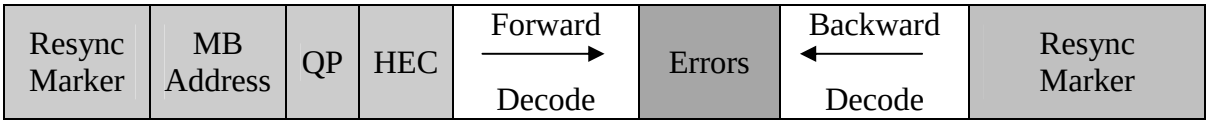

Figure 4: Reversible Variable Length Codes.